



Article

# Flavone and Hydroxyflavones Are Ligands That Bind the Orphan Nuclear Receptor 4A1 (NR4A1)

Miok Lee <sup>1,2</sup>, Srijana Upadhyay <sup>1</sup>, Fuada Mariyam <sup>1</sup>, Greg Martin <sup>1</sup>, Amanuel Hailemariam <sup>1</sup>, Kyongbum Lee <sup>3</sup> , Arul Jayaraman <sup>4</sup>, Robert S. Chapkin <sup>5</sup> , Syng-Ook Lee <sup>6</sup> and Stephen Safe <sup>1,\*</sup>

- <sup>1</sup> Department of Veterinary Physiology and Pharmacology, Texas A&M University, College Station, TX 77843, USA; mi-ok.lee@ag.tamu.edu (M.L.); supadhyay@cvm.tamu.edu (S.U.); fuada@tamu.edu (F.M.); gmartin@tamu.edu (G.M.); ahailemariam@tamu.edu (A.H.)
- <sup>2</sup> Department of Biochemistry and Biophysics, Texas A&M University, College Station, TX 77843, USA
- <sup>3</sup> Department of Chemical and Biological Engineering, Tufts University, Medford, MA 02155, USA; kyongbum.lee@tufts.edu
- <sup>4</sup> Artie McFerrin Department of Chemical Engineering, Texas A&M University, College Station, TX 77843, USA; arulj@mail.che.tamu.edu
- <sup>5</sup> Department of Nutrition, Texas A&M University, College Station, TX 77843, USA; robert.chapkin@ag.tamu.edu
- <sup>6</sup> Department of Food Science and Technology, Keimyung University, Daegu 42601, Republic of Korea; syng-ook.lee@kmu.ac.kr
- \* Correspondence: ssafe@cvm.tamu.edu; Tel.: +1-979-845-5988; Fax: +1-979-862-4929

**Abstract:** It was recently reported that the hydroxyflavones quercetin and kaempferol bind the orphan nuclear receptor 4A1 (NR4A1, Nur77) and act as antagonists in cancer cells and tumors, and they inhibit pro-oncogenic NR4A1-regulated genes and pathways. In this study, we investigated the interactions of flavone, six hydroxyflavones, seven dihydroxyflavones, three trihydroxyflavones, two tetrahydroxyflavones, and one pentahydroxyflavone with the ligand-binding domain (LBD) of NR4A1 using direct-binding fluorescence and an isothermal titration calorimetry (ITC) assays. Flavone and the hydroxyflavones bound NR4A1, and their  $K_D$  values ranged from 0.36  $\mu\text{M}$  for 3,5,7-trihydroxyflavone (galangin) to 45.8  $\mu\text{M}$  for 3'-hydroxyflavone.  $K_D$  values determined using ITC and  $K_D$  values for most (15/20) of the hydroxyflavones were decreased compared to those obtained using the fluorescence assay. The results of binding, transactivation and receptor–ligand modeling assays showed that  $K_D$  values, transactivation data and docking scores for these compounds are highly variable with respect to the number and position of the hydroxyl groups on the flavone backbone structure, suggesting that hydroxyflavones are selective NR4A1 modulators. Nevertheless, the data show that hydroxyflavone-based nutraceuticals are NR4A1 ligands and that some of these compounds can now be repurposed and used to target sub-populations of patients that overexpress NR4A1.

**Keywords:** flavone; hydroxyflavones; binding; NR4A1



**Citation:** Lee, M.; Upadhyay, S.; Mariyam, F.; Martin, G.; Hailemariam, A.; Lee, K.; Jayaraman, A.; Chapkin, R.S.; Lee, S.-O.; Safe, S. Flavone and Hydroxyflavones Are Ligands That Bind the Orphan Nuclear Receptor 4A1 (NR4A1). *Int. J. Mol. Sci.* **2023**, *24*, 8152. <https://doi.org/10.3390/ijms24098152>

Academic Editor: Antonio Lucacchini

Received: 13 April 2023

Revised: 26 April 2023

Accepted: 28 April 2023

Published: 2 May 2023



**Copyright:** © 2023 by the authors. Licensee MDPI, Basel, Switzerland. This article is an open access article distributed under the terms and conditions of the Creative Commons Attribution (CC BY) license (<https://creativecommons.org/licenses/by/4.0/>).

## 1. Introduction

Flavonoids are polyphenolic phytochemicals produced in fruits, nuts, and vegetables, and these compounds share a common phenylchromene-4-one structure substituted with one or more hydroxyl group substituents [1–3]. Dietary consumption of flavone and flavonoid-containing foods is associated with improved health benefits which have been linked to their antioxidant and anti-inflammatory activities and their direct effects on other signaling pathways [4–9]. For example, in the Framingham offspring cohort, “higher long term dietary intakes of flavonoids” and related compounds are associated with a lower risk of Alzheimer’s disease and related dementias [10]. In another study, higher dietary intake of flavonoids was associated with lower rates of obesity [11] and this association was also observed for other health benefits including increased lifespan [12,13]. Flavonoids have

also been used in pre-clinical animal models and in cell culture studies to investigate their chemotherapeutic effects for treating multiple diseases including cancer and non-cancer endpoints such as endometriosis, intestinal inflammation, and neuronal diseases [14–24]. Although the mechanisms of action of flavonoids are complex, in some studies, major contributing flavonoid-induced pathways were identified. For example, several flavonoids interact with the aryl hydrocarbon receptor (AhR), and both cardamonin and baicalein are polyhydroxylated flavonoids that exhibit AhR-dependent inhibition of intestinal inflammatory activity in rodent models [24–27]. Flavonoids also bind other receptors, enzymes, and multiple proteins; however, the mechanisms associated with their chemopreventive, and chemotherapeutic effects are not well-defined [28].

Many nutraceuticals are flavonoid-based products and traditional medicines containing these compounds represent a multibillion-dollar component of the pharmaceutical industry. Although preclinical laboratory studies on flavonoids are promising, the results of human clinical trials with flavones and other flavonoids have been disappointing [24,28]. Moreover, there are major problems with using flavonoids as pharmaceuticals in clinical trials due to their rapid metabolism and poor uptake caused by unfavorable pharmacokinetics/pharmacodynamics. Another problem that contributes to the relative ineffectiveness of flavonoids in clinical trials is the lack of precision in using “flavonoid-based” pharmaceuticals since the cellular targets for flavonoids in patient populations are not well-defined.

Studies in this laboratory have been focused on the orphan nuclear receptors NR4A1 (Nur77) and NR4A2 (Nurr1), which are transiently induced by diverse stressors in normal cells and overexpressed in many stress-related diseases including solid tumors [29–31]. In solid tumors, NR4A1 and NR4A2 are negative prognostic factors, they exhibit pro-oncogenic activities, and these can be inhibited by bis-indole derived compounds (CDIMs) which bind NR4A1 and NR4A2 and act as antagonists in cancer cells [31,32]. These CDIM compounds have minimal effects on NR4A3, and this receptor has not been extensively investigated in solid tumors [31]. Many of the anticancer activities of flavonoids and other polyphenolics resemble those reported for CDIM/NR4A1/2 antagonists and like the antagonists, the flavonoids quercetin and kaempferol also bound NR4A1 and exhibited NR4A1 antagonist activities in rhabdomyosarcoma cells and inhibited tumor growth in an athymic mouse xenograft model [33]. These results observed in Rh30 cells prompted the study reported herein where we show that flavone and several hydroxyl-substituted flavones bind NR4A1 and confirm that this important class of polyphenolics are NR4A1 ligands. The results complement our recent studies on quercetin and kaempferol; however, our structure–NR4A1 binding,  $K_D$  values and structure-dependent transactivation results are poorly correlated. The results suggest that the hydroxyflavones are selective NR4A1 modulators and their agonist or antagonist activities are cell- and gene-context dependent and require individual compound studies on their mode of action and efficacy.

## 2. Results

Recent studies show that polyphenolic compounds such as quercetin, kaempferol, broussonchalcone and resveratrol bind the orphan nuclear receptor NR4A1, and in cancer cell models these compounds act as NR4A1 antagonists [33–35]. In this study, we examined the direct binding of flavone and structurally diverse hydroxyflavones which contained a variable number of hydroxyl groups with different substitution patterns to the ligand-binding domain of NR4A1. We initially used a fluorescent binding assay that measured the quenching of the fluorescence of a Trp residue in the LBD of NR4A1. The binding of selected hydroxyflavones to the LBD of NR4A1 and the calculated  $K_D$  values are shown in Figure 1 and values for all 20 compounds are summarized in Table 1. The fluorescent Trp quenching assay was used to derive the direct binding curve for the 3-, 5-, 6-, 7-, 3'- and 4'-hydroxyflavones. 3-Hydroxyflavone was insoluble in the fluorescence assay and results were inconsistent. The  $K_D$  values for the remaining compounds varied from 45.8 to 1.4  $\mu\text{M}$  for 3'- and 5-hydroxyflavone, respectively. Flavone also bound NR4A1, and the  $K_D$  value was 3.4  $\mu\text{M}$ . We also investigated the direct binding of sev-

eral isomeric dihydroxyflavones to the LBD of NR4A1, and the  $K_D$  values varied from 21.4  $\mu\text{M}$  for 7,3'-dihydroxyflavone to 0.66  $\mu\text{M}$  for 3,6-dihydroxyflavone. There were several interesting changes in the binding affinities between the parent mono-hydroxyflavones and their corresponding dihydroxyflavone analogs where the  $K_D$  values for most of the dihydroxyflavones were lower than those of the corresponding mono-hydroxyflavones. For example,  $K_D$  values for 3'- and 4'-hydroxyflavone were 45.8  $\mu\text{M}$  and 13.0  $\mu\text{M}$ , respectively whereas the  $K_D$  for 3',4'-dihydroxyflavone was 0.96  $\mu\text{M}$ . We also examined  $K_D$  values for the binding of several tri-, tetra- and penta-hydroxyflavones to NR4A1 and they varied from 0.36  $\mu\text{M}$  for 3,5,7-trihydroxyflavone (galangin) to 1.85  $\mu\text{M}$  for 5,6,7-trihydroxyflavone. Inspection of the binding data for the tri-, tetra- and penta-hydroxyflavones showed a range of  $K_D$  values that did not indicate any specific structure–activity relationships among these compounds. Flavones substituted with hydroxyl groups at the 3,5-, 5,7- and 3,5,7-positions in the flavone backbone tended to bind with higher affinity to NR4A1 than their corresponding positional isomers did. However, based on the results summarized in Table 1, the structure–binding relationships between hydroxyflavones and NR4A1 were not apparent.

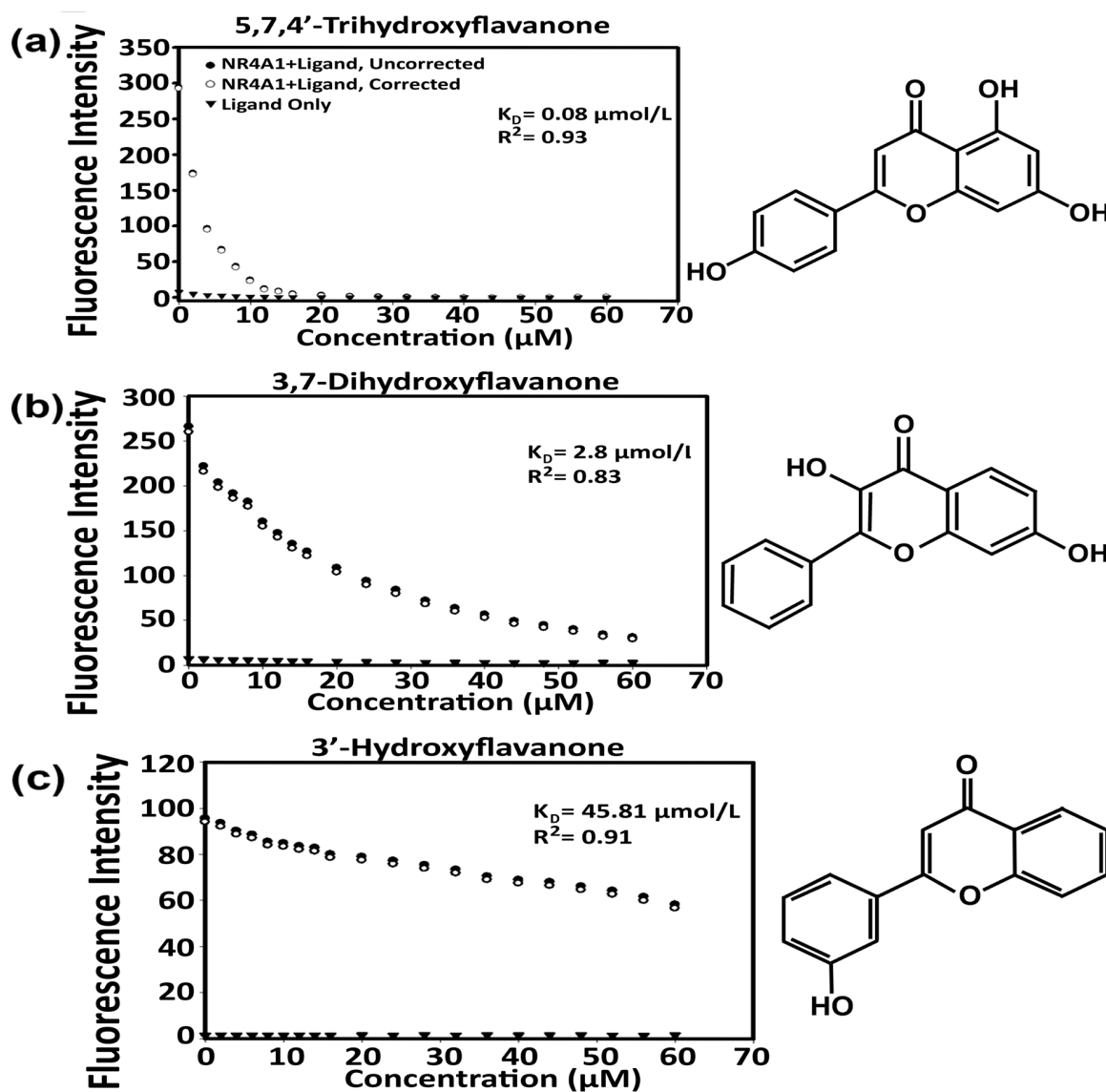


**Figure 1.** Binding of hydroxyflavones to the LBD of NR4A1: fluorescence assay. 5,7,4'-Trihydroxyflavanone (a), 3,7-dihydroxyflavanone (b), and 3'-hydroxyflavanone (c) were incubated with the LBD of NR4A1, binding was determined using a fluorescent binding assay and  $K_D$  and  $R^2$  values were also determined as described [33].

**Table 1.** Binding  $K_D$  values of flavone, hydroxyflavones and naringenin to the ligand-binding domain of NR4A1.

Compound	Direct Binding Assay		ITC Assay	
	$K_D$	$R^2$	$K_d$ , mmol/L	$\Delta G$ , kJ/mol
Flavone	3.4	0.9	0.075	−40.7
3-Hydroxyflavone	N/A *	N/A	0.0225	−43.6
5-Hydroxyflavone	1.4	0.87	18	−27
6-Hydroxyflavone	12.5	0.86	0.032	−42.9
7-Hydroxyflavone	7.4	0.93	0.042	−42.1
3'-Hydroxyflavone	45.8	0.91	0.33	−37
4'-Hydroxyflavone	13.02	0.9	0.15	−39.4
3,6-Dihydroxyflavone	0.66	0.98	444	−19.1
3,7-Dihydroxyflavone	2.8	0.83	0.18	−38.5
5,7 Dihydroxyflavone	11.3	0.89	0.001	−51.3
7,3'-Dihydroxyflavone	21.4	0.89	0.17	−38.7
7,4'-Dihydroxyflavone	9.1	0.68	0.49	−36.1
7,8-Dihydroxyflavone	17.64	0.99	0.042	−42.1
3',4'-Dihydroxyflavone	0.96	0.59	9.5	−28.7
3,5,7 -Trihydroxyflavone (Galangin)	0.36	0.64	0.001	−51.2
5,6,7 -Trihydroxyflavone (Baicalein)	1.85	0.91	0.13	−39.4
5,7,4' -Trihydroxyflavone (Apigenin)	1.77	0.87	0.57	−35.7
3,5,7,4' -Tetrahydroxyflavone (Kaempferol)	3.1	0.95	97.1	−22.9
5,7,3'4' -Tetrahydroxyflavone (Luteolin)	5.1	0.98	0.019	−44.1
3,7,3',4'5' -Pentahydroxyflavone (Quercetin)	0.81	0.97	0.35	−36.8

\* 3-Hydroxyflavone is insoluble. (N/A)

Since the  $K_D$  values obtained using the fluorescence binding assay were highly variable and did not exhibit any consistent structure-dependent effects, we also used the isothermal titration calorimetry (ITC) assay which measures the heat lost or gained due to ligand–NR4A1 binding and this assay provides both  $K_D$  and  $\Delta G$  values associated with these interactions. The results (Table 1) show that  $K_D$  values were highly variable (444 to 0.001  $\mu\text{M}$ ) and did not correlate with the  $K_D$ s obtained using the fluorescence assay. Fifteen of the twenty hydroxyflavones exhibited ITC-derived  $K_D$  values lower than those observed using the fluorescence assay whereas the inverse was true for five of these compounds. Figure 2 illustrates the binding curves and thermodynamic data for 6- and 7-hydroxyflavone. It was noteworthy that some of the  $K_D$  values using the ITC assay were in the low nM range including those for 5,7-dihydroxyflavone ( $K_D = 1$  nM) and 3,5,7-trihydroxyflavone ( $K_D = 1$  nM), and there was rank order correlation among the hydroxyflavones between their  $K_D$  and  $\Delta G$  values as determined by the ITC binding assay. There was no obvious explanation for the in vitro assay-dependent differences in  $K_D$  values from the two binding assays except that the ITC assay integrated ligand binding not only within the ligand-binding domain but also on other surfaces of the receptor.

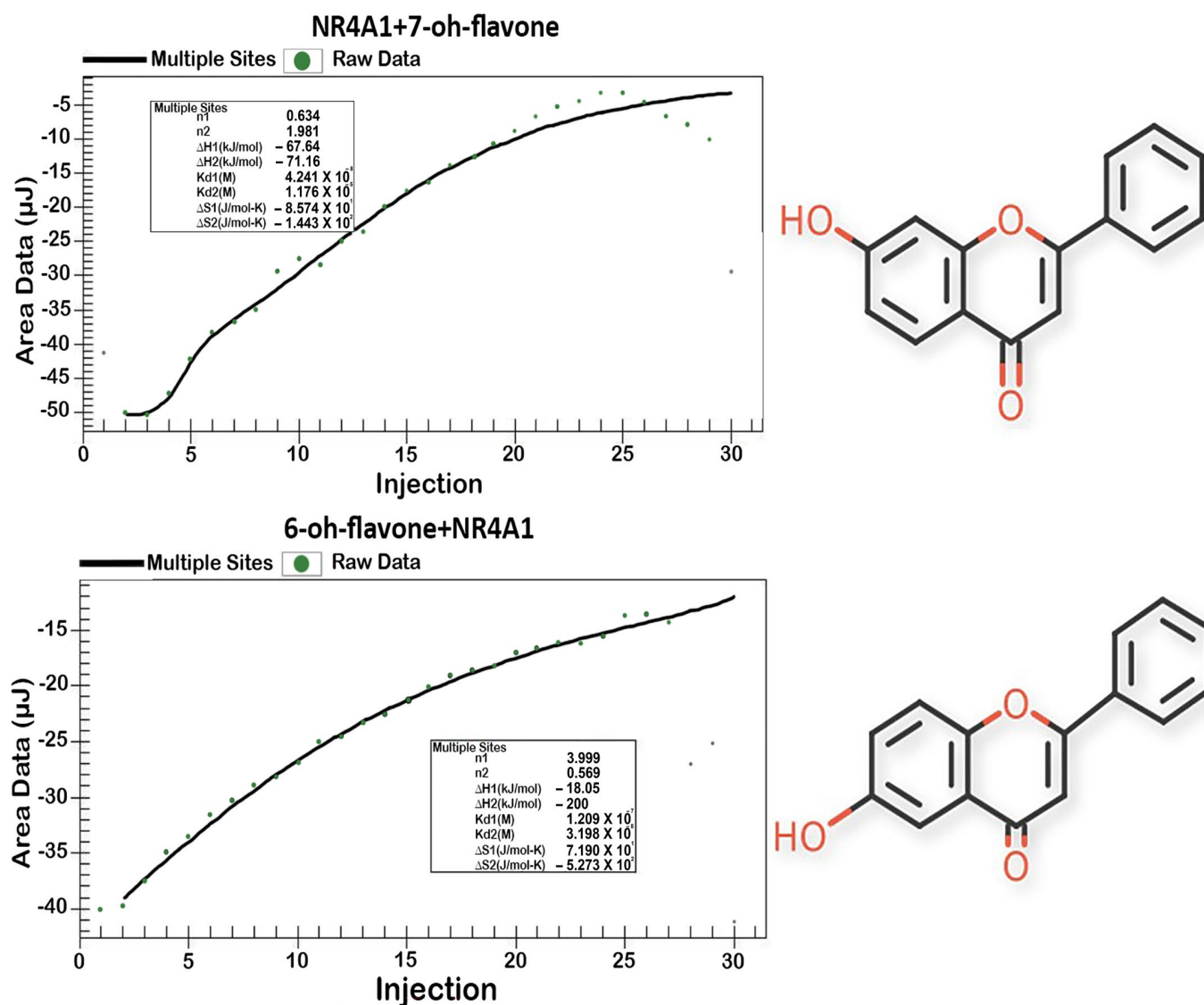


**Figure 2.** Binding of hydroxyflavones to the LBD of NR4A1: ITC assay. Interactions of 6-hydroxyflavone and 7-hydroxyflavone with the LBD of NR4A1 were determined using an Affinity ITC and analysis of the  $K_D$ , and thermodynamic data were obtained as described using a data analysis software package supplied by the manufacturer.

We also examined the effects of flavone and the hydroxyflavones on NR4A1-dependent transactivation in Panc1 pancreatic cancer cells transfected with GAL4-NR4A1/UAS-luc constructs (Figure 3). Cells were treated with 25 or 50  $\mu\text{M}$  concentrations of the flavones and the effects on luciferase activity were variable; 4'-hydroxy-, 6-hydroxy-, 7-hydroxy-, 5,6,7-trihydroxy-, 5,7,3',4'-tetrahydroxy- and 3,5,7,3',4'-pentahydroxyflavone (quercetin) significantly induced luciferase activity. In contrast, only 3,5,7-trihydroxyflavone decreased luciferase activity; the remaining hydroxyflavones increased or decreased luciferase activity but these responses were not significant. We observed minimal toxicity using these flavone concentrations (<20% floating cells) and this was consistent with our previous studies on their AhR-dependent activities [36,37]. These results contrasted those of previous studies using quercetin (3,5,7,3',4'-pentahydroxyflavone) and kaempferol (3,4',5,7-tetrahydroxyflavone), which decreased luciferase activity in Rh30 rhabdomyosarcoma cells transfected with the same constructs [33]; in contrast, the results obtained in Panc1 cells were highly variable. It is possible that higher concentrations (>50  $\mu\text{M}$ ) are required to elicit

induced or inhibited transactivation; however, these higher concentrations were not used due to the toxicities of these compounds at higher concentrations.

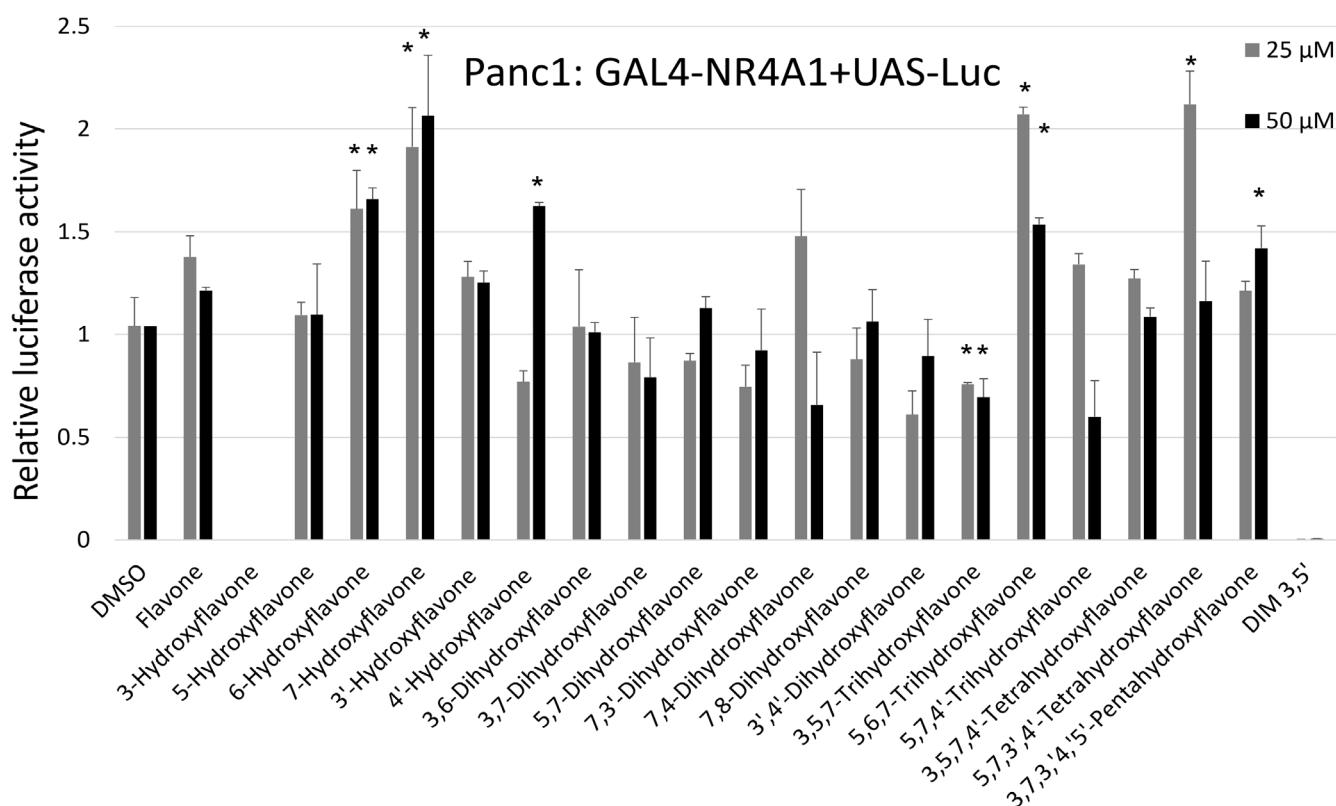


**Figure 3.** Hydroxyflavonoid activation of NR4A1-dependent transactivation. Panc1 cells were cotransfected with GAL4-NR4A1 and UAS-luciferase constructs, cells were treated with 25 and 50 μM hydroxyflavonoids and luciferase activity (normalized to β-galactosidase activity) was determined. Results were determined in triplicate for each concentration and are plotted as mean values ± SE. Significant induction or inhibition ( $p < 0.05$ ) of luciferase activity is illustrated (\*).

Based on these variable results from Panc1 cells, we repeated the NR4A1-dependent transactivation assays in Rh30 cells using a high concentration (50 μM) that was not cytotoxic. Both kaempferol and quercetin decreased transactivation as previously reported in this cell line [33] and similar results were observed for 1,1-bis(3'-indolyl)-1-(3,5-dichlorophenyl)methane (DIM-3,5-Cl<sub>2</sub>) which is a highly potent bis-indole-derived NR4A1 antagonist [32] that was used as a control for this assay. There were more distinct differences between the hydroxyflavones that inhibited transactivation in Rh30 cells compared to those observed in Panc1 cells and potent inhibition was observed for 4'-hydroxy, 3,6-dihydroxy, 3,7-dihydroxy, 3,5,7-trihydroxy and 3,5,3',4'-tetrahydroxyflavone (Figure 4). Moreover, 6-hydroxy, 5,6,7-trihydroxy and 5,7,4'-trihydroxyflavone also decreased transactivation in Rh30 cells whereas the remaining compounds did not increase or slightly increased transactivation in Rh30 cells. Interestingly, 7-hydroxy and 3',4'-dihydroxyflavone induced (<2.4-fold) luciferase activity in both cell lines. The results obtained for Rh30 cells were more definitive than those observed for Panc1 cells in terms of identifying hydroxyflavones that inhibited NR4A1-dependent transactivation, but structure–activity relationships were not observed.

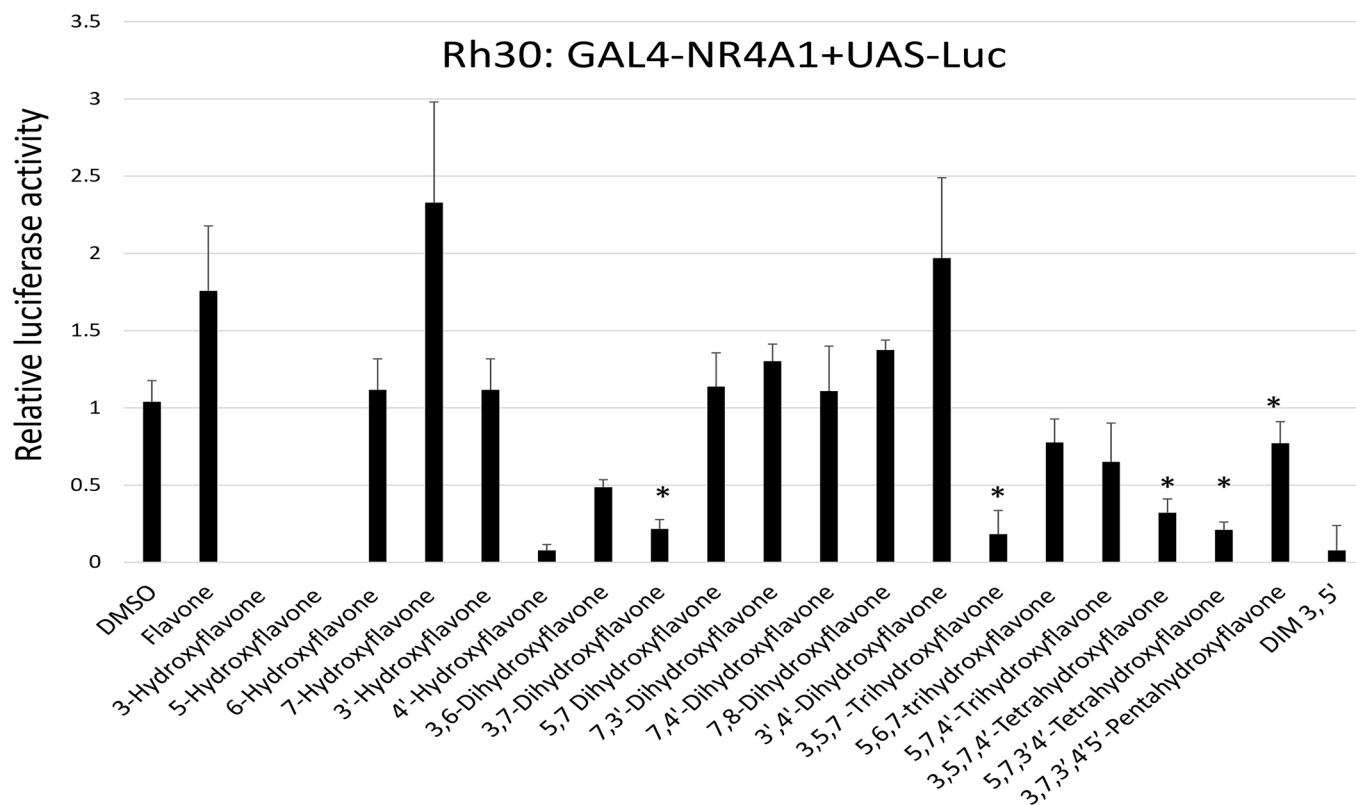


**Figure 4.** Hydroxyflavonoid activation of NR4A1-dependent transactivation. Rh30 cells were co-transfected with GAL4-NR4A1 and UAS-luciferase constructs, cells were treated with 50  $\mu$ M hydroxyflavones and luciferase activity (normalized to  $\beta$ -galactosidase activity) was determined. Results were determined in triplicate for each concentration and are plotted as mean values  $\pm$ SE. Significant induction or inhibition ( $p < 0.05$ ) of luciferase activity is illustrated (\*).

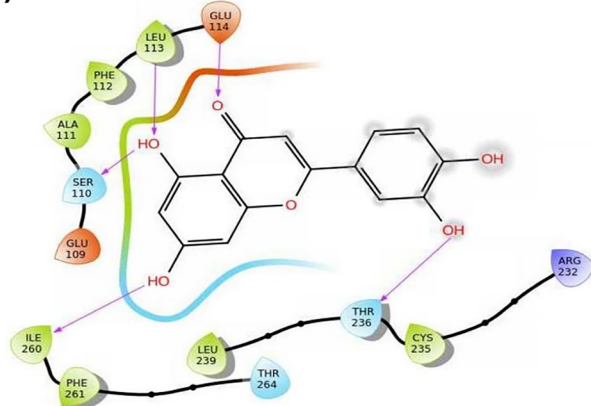
We also carried out modeling studies using Maestro/Schrodinger software on the interaction of flavones/hydroxyflavones with TMY301 and TMY302 sites in the LBD of NR4A1 (3V3Q) [38]. The docking scores for interactions of hydroxyflavones at site TMY301 and TMY302 are summarized in Table 2 and Supplemental Figure S1. The results show that, with the exception of 3,6-dihydroxyflavone, the docking scores indicated that the remaining hydroxyflavones more favorably interacted with site TMY301 than they did with site TMY302. The variation in docking scores for site TMY301 ranged from  $-7.059$  (5,7,3',4'-tetrahydroxyflavone) to  $-4.695$  (3,7-dihydroxyflavone) and those for site TMY302 ranged from  $-5.85$  (3,7-dihydroxyflavone) to  $-4.582$  (flavone). Figure 5 illustrates the interactions of the compounds that bind with the highest and lowest affinities to TMY301 and TMY302 in the LBD of NR4A1. Previous studies show that ethyl 2-[2,3,4-trimethoxy-6-(octanoyl)phenyl] acetate also binds both sites, which are close to the surface of the ligand pocket, and the docking scores for these sites are  $-4.83$  and  $-5.62$ , respectively, showing a preference for TMY302. The results indicate that flavone and the hydroxyflavones interact with both sites in the LBD of NR4A1 with preferential binding to TMY301 (exception: 3,6-dihydroxyflavone). An examination of the docking scores,  $K_D$  values for two assays and  $-\Delta G$  values did not show any obvious structure-binding or structure-docking relationships and this was consistent with the lack of structure-activity (transactivation) correlations. Many of the early studies on high-affinity ligands such as steroid hormones and their binding to corresponding cognate receptors exhibit structure-activity relationships. However, subsequent development of lower-affinity receptor ligands for nuclear receptors such as the estrogen receptor  $\alpha$  (ER $\alpha$ ) do not necessarily exhibit structure-activity relationships; this is illustrated by selective ER modulators (SERMs) which have and are being developed

for hormonal therapies [39,40]. Thus, results of this study suggest that hydroxyflavones may also be selective NR4A1 modulators and this is further discussed below.

**Table 2.** Summary of docking scores for flavone and hydroxyflavones from modeling studies.

Compound	Site TMY301: Docking Score kcal/mol	Site TMY302: Docking Score kcal/mol
Flavone	−5.741	−4.582
3-Hydroxyflavone	−5.507	−4.716
5-Hydroxyflavone	−6.302	−4.732
6-Hydroxyflavone	−5.619	−5.4
7-Hydroxyflavone	−5.878	−5.477
3'-Hydroxyflavone	−6.756	−5.176
4'-Hydroxyflavone	−5.861	−4.717
3,6-Dihydroxyflavone	−4.695	−5.51
3,7-Dihydroxyflavone	−5.934	−5.851
5,7-Dihydroxyflavone	−6.399	−5.543
7,3'-Dihydroxyflavone	−6.719	−5.559
7,4'-Dihydroxyflavone	−5.575	−5.42
7,8-Dihydroxyflavone	−5.941	−5.049
3',4'-Dihydroxyflavone	−5.736	−5.507
3,5,7-Trihydroxyflavone (Galangin)	−6.791	−4.83
5,6,7-Trihydroxyflavone (Baicalein)	−5.711	−5.711
5,7,4'-Trihydroxyflavone (Apigenin)	−6.441	−4.782
3,5,7,4'-Tetrahydroxyflavone (Kaempferol)	−6.555	−5.433
5,7,3',4'-Tetrahydroxyflavone (Luteolin)	−7.059	−5.832
3,7,3',4',5'-Pentahydroxyflavone (Quercetin)	−6.437	−5.397
4',5,7-Trihydroxyflavone (Naringenin)	−6.618	−5.656
Binding Pocket Residues	GLU114, LEU113, PHE112, ALA111, SER110, GLU109, LEU108, ILE260, PHE261, THR264, PRO266, LEU239, THR236, CYS235, ARG232, ARG184, VAL179	HIE41, LEU42, ASP43, SER44, GLY45, PRO46, SER47, THR48, LEU51, ILE132, LYS125, ARG123, TYR122, ARG119, LEU162, HIE163, LEU165, LEU166, VAL167, VAL169, PHE172

(a) 3V3Q:TM301 - 5,7,3',4'-Tetrahydroxyflavone (Luteolin)

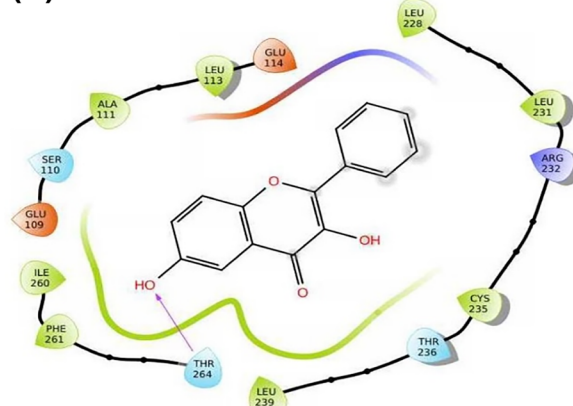


$K_D = 5.1 \mu\text{M}$

Docking Score =  $-7.059 \text{ kcal/mol}$

Amino Acid Residues: Glu114, Leu113, Phe112, Ala111, Ser110, Glu109, Phe261, Thr264, Leu239, Thr236, Cys235, and Arg232

(b) 3V3Q:TM301 - 3,6-Dihydroxyflavone

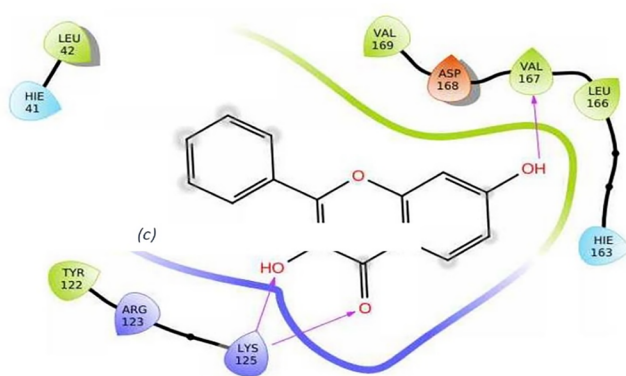


$K_D = 0.66 \mu\text{M}$

Docking Score =  $-4.695 \text{ kcal/mol}$

Amino Acid Residues: Glu114, Leu113, Phe112, Ala111, Ser110, Glu109, Ile260, Phe261, Thr264, Leu239, Thr236, Cys235, Arg232, Leu231, and Leu228

(c) 3V3Q:TM302 - 3,7-Dihydroxyflavone

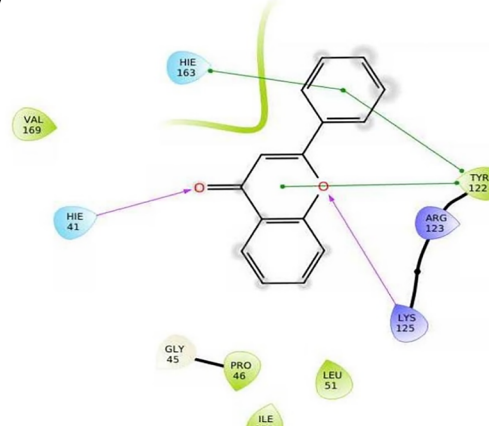


$K_D = 2.8 \mu\text{M}$

Docking Score =  $-5.934 \text{ kcal/mol}$

Amino Acid Residues: Hie41, Leu42, Lys125, Arg123, Tyr122, Hie163, Leu166, Val167, and Val169

(d) 3V3Q:TM302 - Flavone



$K_D = 3.4 \mu\text{M}$

Docking Score =  $-4.582 \text{ kcal/mol}$

Amino Acid Residues: Hie41, Gly45, Pro46, Leu51, Lys125, Arg123, Tyr122, Hie163, and Val169

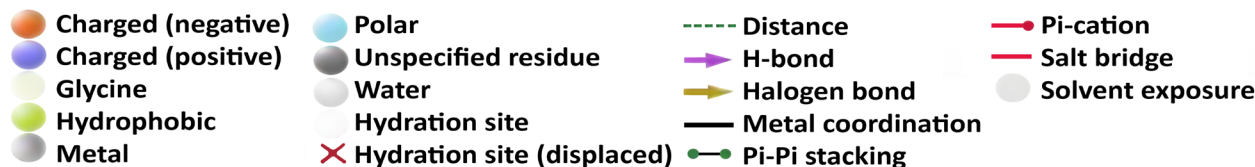


Figure 5. Modeling of hydroxyflavone binding to NR4A1. Modeling studies were carried out as described in the Methods and interactions of 5,7,3',4'-tetrahydroxyflavone (a) and 3,6-dihydroxyflavone (b) gave docking scores of  $-5.1$  and  $-4.695$ , respectively to TM301. Interactions with amino acids are indicated. The docking scores of 3,7-dihydroxyflavone (c) and flavone (d) were  $-5.934$  and  $-4.582$ , respectively to TM302. The types of interactions include: hydrophobic (green), polar (light blue), positively charged (dark blue), negatively charged (red/orange), hydrogen bonding (purple).

### 3. Discussion

The orphan nuclear receptors NR4A1, NR4A2 and NR4A3 are overexpressed in multiple diseases including solid tumors [31] where both NR4A1 and NR4A2 act as pro-oncogenic factors. In contrast, based on the results of NR4A1 and NR4A3 knockout studies on mice, it was shown that the dual knockdown of both NR4A1 and NR4A3 in mice resulted in the development of leukemia, and NR4A1 and NR4A3 exhibited tumor suppressor-like activities in most blood-derived tumors [41,42]. Many studies have focused on the role and functions of orphan NR4A and there is now a growing body of literature on the identification and functions of these receptors, although endogenous NR4A ligands have not been identified. Compounds that bind NR4A1 and NR4A2 have been reported whereas less is known about ligands that bind NR4A3 [29–31]. Interestingly, many of the initial compounds identified as NR4A1 or NR4A2 ligands are natural products and some of them serve as scaffolds for the synthesis of more potent analogs [43,44]. For example, phytochemicals/microbial metabolites that bind NR4A1 include cytosporone B, celastrol, fangchinoline, isoalantolactone, polyunsaturated fatty acids, a bacterial bile acid metabolite, quercetin and kaempferol, a sponge-derived sesterterpenoid 12-deacetyl-12-epi-scalaradial and prostaglandin A2 [33–35,43,45–51]. NR4A2 also binds natural products including prostaglandins E1 and A1, 5,6-dihydroxyindole (a dopamine metabolite) and unsaturated fatty acids [49–55]. Interestingly the only compounds reported to bind both NR4A1 and NR4A2 are the unsaturated fatty acids and arachidonic acid and docosahexaenoic acid bind both receptors [51,54].

Kaempferol and quercetin are ligands that bind NR4A1 and exhibit NR4A1 antagonist activities in Rh30 rhabdomyosarcoma cells [33] and this has previously been observed for other NR4A1 antagonist such as the bis-indole derived compounds that also bind NR4A1 [31]. Since many flavonoids exhibit anticancer activities [23,56,57] similar to those observed with kaempferol and quercetin, we further investigated flavone and hydroxyflavones as potential ligands for NR4A1. Many of these flavonoids are extensively used as nutraceuticals and traditional medicines worldwide; however, their application as precision medicines has been limited since their mechanisms of action and specific intracellular targets are not fully understood or identified. We initially examined these compounds as ligands for NR4A1 using a direct binding assay which measures the loss of fluorescence associated with a tryptophan residue in the ligand-binding domain of the receptor [33]. Flavone itself bound NR4A1 with a  $K_D$  of 3.4  $\mu\text{M}$ , and among the hydroxyflavone isomers examined only 5-hydroxyflavone exhibited a lower  $K_D$  (1.4  $\mu\text{M}$ ) than flavone did and 3'-hydroxyflavone exhibited the lowest binding affinity with a  $K_D$  value of 45.8  $\mu\text{M}$ . Binding studies with 3-hydroxyflavone gave unreliable results due to the aqueous insolubility of this compound. Subsequent binding of hydroxyflavones to NR4A1 and their corresponding  $K_D$  values were highly variable among several di-pentahydroxy flavones and ranged from 0.36  $\mu\text{M}$  for 3,5,7-trihydroxyflavone (galangin) to 16.4  $\mu\text{M}$  for 3,4,7'-trihydroxyflavone.  $K_D$  and  $\Delta G$  values were also determined for the hydroxyflavones using the ITC binding assay and for 15/20 of these compounds, lower  $K_D$  values were observed in the ITC vs. the fluorescence binding assay (Table 1). Although the  $K_D$  and  $\Delta G$  values were correlated in the ITC assay, there were no obvious structure-binding/activity relationships using this assay and correlations between the two different sets of  $K_D$  values for the hydroxyflavones were not observed.

Molecular modeling studies using Maestro/Schrodinger software investigated interactions of the hydroxyflavones with amino acid side chains in the LBD of NR4A1 (Table 2), and Figure 5 illustrates the interactions of 5,7,3',4'-tetrahydroxyflavone compared to those of 3,6-dihydroxyflavone in the NR4A1-TMY301 binding site and the interactions of 3,7-dihydroxyflavone and flavone in the NR4A1-TMY302 binding site. These compounds have the lowest and highest docking values for each binding site; for each binding site there is considerable overlap in their interactions with common amino acid side chains but also differences which presumably dictate the differences in their docking scores. It is also apparent that different sets of amino acids are important for the interactions of the flavonoids

with the TMY301 and TMY302 binding sites. However, there was also no correlation between the  $K_D$  values and docking scores for the compounds illustrated in Figure 5 and other hydroxyflavones listed in Table 2. Thus, the binding and modeling studies do not identify structure–activity relationships that correlate with  $K_D$  values observed in the direct fluorescence and ITC binding assays.

We also examined the effects of the flavones on NR4A1-dependent transactivation using a GAL4-NR4A1 chimera and UAS-luc constructs and observed that ligand dependency increased, decreased and had no effect on luciferase activity. Previous studies showed that quercetin and kaempferol acted as NR4A1 antagonists in Rh30 rhabdomyosarcoma cells [33] and decreased NR4A1-dependent transactivation in this cell line. Our initial studies showed some variation in the effects of hydroxyflavonoids on NR4A1-dependent luciferase activity in Panc1 cells which appeared to be relatively resistant to the effects of hydroxyflavones as either agonists or antagonists using the GAL4/UAS-luc assay. In contrast, several hydroxyflavones were NR4A1 antagonists in Rh30 cells and this was consistent with previous studies with quercetin and kaempferol which also exhibited functional activity as NR4A1 antagonists in Rh30 cells [33]. This suggests that hydroxyflavones may be selective NR4A1 modulators and that the effects of individual compounds may be cell context-, response- and gene-specific. This selectivity is observed for many nuclear receptor ligands and their receptors [39,40,58]. For example, selective estrogen receptor modulators (SERMs) such as fasoldex, tamoxifen and raloxifene exhibit different  $K_D$  values for ER binding, and among structurally diverse estrogenic compounds their  $K_D$  values and response selectivities are also highly variable [39].

Thus, our results did not show any structure– $K_D$  (binding), structure–activity (trans-activation), or structure–docking relationships for twenty flavonoids using two complementary binding assays and two transactivation assays and by modeling interactions with NR4A1. The addition of more flavones may be needed to resolve some of these issues; however, examinations of previous structure–binding and structure–activity relationships of flavonoids with other receptors gave similar results which precluded the development of structure–potency correlations. Studies in this laboratory on structure–activity relationships for hydroxyflavones as AhR agonists and antagonists also gave highly variable results. Although  $K_D$  values for hydroxyflavone–AhR binding were not determined, the effects of hydroxyflavones as inducers of AhR-responsive CYP1A1, CYP1B1 and UGT1A1 genes were determined in Caco2 cells [36,37]. There were some structure-dependent effects among the disubstituted flavones where most 6-substituted dihydroxyflavones were agonists and 7-substituted dihydroxyflavones were antagonists of CYP1A1 induction. However, both 6- and 7-substituted dihydroxyflavones were AhR agonists for the induction of CYP1B1 [36], and for more highly substituted hydroxyflavones, substituent effects on activity were not observed. The lack of predictive structure–activity relationships of hydroxyflavones as AhR ligands was also summarized in a recent review which clearly demonstrates the cell context- and response-dependent variability of hydroxyflavones as AhR agonists and antagonists [25]. Another study used modeling to determine the docking scores of flavonoids for several receptors. For example, the docking values of 17 $\beta$ -estradiol, 5,7,4'-trihydroxyflavone (apigenin), 5,7,3',4'-tetrahydroxyflavone (luteolin) and 3,7,3',4',5-pentahydroxyflavone (quercetin) for ER $\alpha$  were  $-10.944$ ,  $-9.698$ ,  $-9.311$  and  $-8.911$ , respectively [59]. Functional studies were not determined; however, another report showed that 5,7,4'-trihydroxyflavone exhibited both ER binding and functional activity whereas quercetin did not bind ER $\alpha$  [60]. It was concluded that “the way in which these molecules exert an agonist or antagonist effect on nuclear receptors is not easily predictable and it likely depends on the specific co-activator/co-repressor population of different tissues” [59]. These results parallel the effects observed for hydroxyflavones in this study, indicating that for NR4A1 the hydroxyflavones are also selective receptor modulators. This implies that clinical applications of specific hydroxyflavones cannot necessarily be derived from structure–binding results but must be individually evaluated and optimized in preclinical studies prior to clinical applications.

## 4. Materials and Methods

### 4.1. Chemicals and Cell Culture

All the hydroxyflavones and flavone were purchased from Indofine Chemical Co. (Hillsbrough, NJ, USA); the purities for a 7,3',4'-, 3,7,3'-, and 5,7,4'-trihydroxyflavone were 97% and all remaining compounds were 98–99% pure. Cancer cells were maintained in Dulbecco's modified Eagle's medium (DMEM) nutrient mixture with Ham's F-12 (DMEM/F-12; Sigma-Aldrich, St. Louis, MO, USA) supplemented with 5% fetal bovine serum (FBS; Sigma-Aldrich) and a 10 mL/L 100× antibiotic–antimycotic solution (Gibco, Thermo Fisher Scientific, Waltham, MA, USA). Cells were maintained at 37 °C in the presence of 5% CO<sub>2</sub>. The 3,5-disubstituted CDIM was synthesized in our laboratory [32].

### 4.2. Plasmids and Luciferase Assay

The UAS-luciferase reporter gene containing 5 GAL4 binding sites and the GAL4-NR4A1 chimera containing the GAL4 DNA-binding domain which linked to the ligand-binding domain (LBD) of NR4A1 were used in transactivation assays in Panc1 pancreatic cancer cells. Panc-1 cells were plated in a 24-well plate (3 × 10<sup>4</sup> cells/well) and grown for 24 h. Cells were then co-transfected with each construct (250 ng) and the β-gal expression construct (25 ng) using GeneJuice (Novagen, Madison, WI, USA) in accordance with the manufacture's protocol. The medium was removed after 18 h and replaced with a 2.5% charcoal-stripped FBS-supplemented medium containing either DMSO or flavonoids (25 and 50 μM) in DMSO. After 24 h, cells were then lysed, and cell extracts were processed to measure luciferase activity. Luciferase activity was normalized by dividing the β-gal expression and each treatment was determined in three independent experiments. Data were expressed as mean ± SE and significant (*p* < 0.05) effects were noted.

### 4.3. Quenching of NR4A1 Tryptophan Fluorescence by Direct Ligand Binding

Tryptophan fluorescence spectra were obtained essentially as described [33]. Briefly, the ligand-binding domain of NR4A1 at the final concentration of 0.5 μmol/L in 1.0 mL of phosphate-buffered saline (PBS, pH 7.4) was used for fluorescence measurements. The protein was incubated for 3 min at 25 °C in a temperature-controlled (Quantum Northwest TC125) fluorescence spectrophotometer (Varian Cary Eclipse). The fluorescence spectra were obtained using an excitation wavelength of 285 nm (excitation slit width = 5 nm) and an emission wavelength range of 300–420 nm (emission slit width = 5 nm). Aliquots (0.1 μL/aliquot) of the ligand (10 mmol ligand/L ethanol) were then added to the cuvette containing NR4A1 to reach a final ligand concentration of up to 60 μmol/L. After each aliquot of the ligand, the NR4A1/ligand solution was incubated at 25 °C for 3 min and the loss of tryptophan fluorescence was measured as described above. The addition of DMSO only (up to a final volume of 3.0 μL) had no effect on NR4A1 tryptophan fluorescence. Ligand binding to NR4A1 was determined by measuring the NR4A1 tryptophan fluorescence intensity at the emission wavelength of 330 nm and the resulting data were used to calculate *K<sub>D</sub>* values. Fluorescence intensity at each ligand concentration was used to correct the NR4A1 tryptophan fluorescence intensity as described [33].

### 4.4. Isothermal Titration Calorimetry

Isothermal titration calorimetry (ITC) was used to determine the ligand-binding constant (*K<sub>D</sub>*) for binding to NR4A1 utilizing an Affinity ITC (TA Instruments, New Castle, DE, USA). Briefly, the experimental setup was as follows. The ITC sample cell contained 250 μL of NR4A1 protein (ligand-binding domain: LBD) at a concentration of 20 μmol/L in a buffer containing 20 mmol sodium phosphate/L (pH 7.4), 5% glycerol, and 1.0% ethanol. The ligand titrant was prepared in the same buffer as that above at a ligand concentration of 100 μmol/L. The initial ligand stock solution was prepared at a final concentration of 10 mmol ligand/L ethanol prior to the preparation of the ligand titrant. Ligand titration into protein was performed at 25 °C with a stir rate of 125 rpm. Each ligand injection volume was 5 μL followed by a duration of 200 s to measure the total heat flow required

to maintain constant temperature. A total of thirty injections were carried out for each ligand/NR4A1 combination. In a separate set of injections, the same ligand dilution was placed into the buffer. The ligand/buffer values were subtracted from the ligand/protein values prior to data analysis using the Affinity ITC manufacturer-supplied data analysis software package. The resulting data are plotted as heat flow ( $\mu$ J) versus the molar ratio of the injected ligand to NR4A1 in the sample cell.

#### 4.5. Computation-Based Molecular Modeling Studies

Molecular modeling studies were conducted using Maestro (Schrödinger Release 2021-3, Schrödinger, LLC, New York, NY, USA, 2021). The version of Maestro used for these studies was licensed to the Laboratory for Molecular Simulation (LMS), a Texas A&M University core-user facility for molecular modeling which is associated with the Texas A&M University's High Performance Research Computing (HPRC) facility (College Station, TX 77843, USA). All Maestro-associated applications were accessed via the graphical user interface (GUI)'s VNC interactive application through the HPRC OnDemand portal. The crystal structure coordinates for the human orphan nuclear receptor NR4A1 ligand-binding domain (LBD) were downloaded from Protein Data Bank (<http://www.fcsb.org>, accessed on 26 April 2023. PDB ID 3V3Q). The human NR4A1 LBD crystal structure was prepared for ligand docking utilizing Maestro Protein Preparation Wizard; restrained minimization of the protein structure was performed utilizing the OPLS4 force field. The three-dimensional structure of each ligand was prepared for docking utilizing Maestro LigPrep. Maestro Glide [61–63] was utilized with the default settings to dock each prepared ligand to each prepared protein, predict the lowest energy ligand-binding orientation, and calculate the predicted binding energy in units of kcal/mol.

**Supplementary Materials:** The following supporting information can be downloaded at: <https://www.mdpi.com/article/10.3390/ijms24098152/s1>.

**Author Contributions:** Conceptualization, S.S.; investigation, M.L., S.U., F.M. and G.M.; data curation, A.H., K.L., A.J., R.S.C. and S.-O.L.; writing—original draft preparation, all authors; writing—review and editing, all authors; funding acquisition, S.S. All authors have read and agreed to the published version of the manuscript.

**Funding:** This research was partially supported by grants from the Syd Kyle chair endowment and the National Institutes of Health (RO1-AT010282 and P30-ES029607).

**Institutional Review Board Statement:** An Institutional Review Board statement is not applicable to these in vitro studies.

**Informed Consent Statement:** Not applicable.

**Data Availability Statement:** The data that support the findings of this study are available from the corresponding author upon reasonable request.

**Conflicts of Interest:** The authors declare no conflict of interest.

## References

1. Panche, A.N.; Diwan, A.D.; Chandra, S.R. Flavonoids: An overview. *J. Nutr. Sci.* **2016**, *5*, e47. [[CrossRef](#)]
2. Křížová, L.; Dadáková, K.; Kašparovská, J.; Kašparovský, T. Isoflavones. *Molecules* **2019**, *24*, 1076. [[CrossRef](#)]
3. Alseekh, S.; de Souza, L.P.; Benina, M.; Fernie, A.R. The style and substance of plant flavonoid decoration; towards defining both structure and function. *Phytochemistry* **2020**, *174*, 112347. [[CrossRef](#)] [[PubMed](#)]
4. Hung, H.C.; Joshipura, K.J.; Jiang, R.; Hu, F.B.; Hunter, D.; Smith-Warner, S.A.; Colditz, G.A.; Rosner, B.; Spiegelman, D.; Willett, W.C. Fruit and vegetable intake and risk of major chronic disease. *J. Natl. Cancer Inst.* **2004**, *96*, 1577–1584. [[CrossRef](#)] [[PubMed](#)]
5. Murillo, G.; Mehta, R.G. Cruciferous vegetables and cancer prevention. *Nutr. Cancer* **2001**, *41*, 17–28. [[CrossRef](#)] [[PubMed](#)]
6. Key, T.J. Fruit and vegetables and cancer risk. *Br. J. Cancer* **2010**, *104*, 6–11. [[CrossRef](#)]
7. Rodríguez-García, C.; Sánchez-Quesada, C.; Gaforio, J.J. Dietary Flavonoids as Cancer Chemopreventive Agents: An Updated Review of Human Studies. *Antioxidants* **2019**, *8*, 137. [[CrossRef](#)] [[PubMed](#)]

8. Liu, Y.; Weng, W.; Gao, R.; Liu, Y. New Insights for Cellular and Molecular Mechanisms of Aging and Aging-Related Diseases: Herbal Medicine as Potential Therapeutic Approach. *Oxidative Med. Cell. Longev.* **2019**, *2019*, 4598167. [[CrossRef](#)] [[PubMed](#)]
9. Bondonno, N.P.; Dalgaard, F.; Kyrø, C.; Murray, K.; Bondonno, C.P.; Lewis, J.R.; Croft, K.D.; Gislason, G.; Scalbert, A.; Cassidy, A.; et al. Flavonoid intake is associated with lower mortality in the Danish Diet Cancer and Health Cohort. *Nat. Commun.* **2019**, *10*, 3651. [[CrossRef](#)] [[PubMed](#)]
10. Shishtar, E.; Rogers, G.T.; Blumberg, J.B.; Au, R.; Jacques, P.F. Long-term dietary flavonoid intake and risk of Alzheimer disease and related dementias in the Framingham Offspring Cohort. *Am. J. Clin. Nutr.* **2020**, *112*, 343–353. [[CrossRef](#)]
11. Marranzano, M.; Ray, S.; Godos, J.; Galvano, F. Association between dietary flavonoids intake and obesity in a cohort of adults living in the Mediterranean area. *Int. J. Food Sci. Nutr.* **2018**, *69*, 1020–1029. [[CrossRef](#)] [[PubMed](#)]
12. Kim, Y.; Je, Y. Flavonoid intake and mortality from cardiovascular disease and all causes: A meta-analysis of prospective cohort studies. *Clin. Nutr. ESPEN* **2017**, *20*, 68–77. [[CrossRef](#)]
13. Pounis, G.; Costanzo, S.; Bonaccio, M.; Di Castelnuovo, A.; de Curtis, A.; Ruggiero, E.; Persichillo, M.; Cerletti, C.; Donati, M.B.; de Gaetano, G.; et al. Reduced mortality risk by a polyphenol-rich diet: An analysis from the Moli-sani study. *Nutrition* **2018**, *48*, 87–95. [[CrossRef](#)] [[PubMed](#)]
14. Yu, J.; Bi, X.; Yu, B.; Chen, D. Isoflavones: Anti-Inflammatory Benefit and Possible Caveats. *Nutrients* **2016**, *8*, 361. [[CrossRef](#)] [[PubMed](#)]
15. Kikuchi, H.; Yuan, B.; Hu, X.; Okazaki, M. Chemopreventive and anticancer activity of flavonoids and its possibility for clinical use by combining with conventional chemotherapeutic agents. *Am. J. Cancer Res.* **2019**, *9*, 1517–1535.
16. Sharma, S.; Naura, A.S. Potential of phytochemicals as immune-regulatory compounds in atopic diseases: A review. *Biochem. Pharmacol.* **2020**, *173*, 113790. [[CrossRef](#)]
17. Oteiza, P.; Fraga, C.; Mills, D.; Taft, D. Flavonoids and the gastrointestinal tract: Local and systemic effects. *Mol. Asp. Med.* **2018**, *61*, 41–49. [[CrossRef](#)] [[PubMed](#)]
18. Salaritabar, A.; Darvishi, B.; Hadjiakhoondi, F.; Manayi, A.; Sureda, A.; Nabavi, S.F.; Fitzpatrick, L.R.; Bishayee, A. Therapeutic potential of flavonoids in inflammatory bowel disease: A comprehensive review. *World J. Gastroenterol.* **2017**, *23*, 5097–5114. [[CrossRef](#)]
19. Algieri, F.; Rodriguez-Nogales, A.; Rodriguez-Cabezas, M.E.; Risco, S.; Ocete, M.A.; Galvez, J. Botanical Drugs as an Emerging Strategy in Inflammatory Bowel Disease: A Review. *Mediat. Inflamm.* **2015**, *2015*, 179616. [[CrossRef](#)]
20. Park, S.; Song, G.; Lim, W. Myricetin inhibits endometriosis growth through cyclin E1 down-regulation in vitro and in vivo. *J. Nutr. Biochem.* **2020**, *78*, 108328. [[CrossRef](#)]
21. Park, S.; Lim, W.; Bazer, F.W.; Whang, K.-Y.; Song, G. Quercetin inhibits proliferation of endometriosis regulating cyclin D1 and its target microRNAs in vitro and in vivo. *J. Nutr. Biochem.* **2018**, *63*, 87–100. [[CrossRef](#)] [[PubMed](#)]
22. Wang, C.C.; Xu, H.; Man, G.C.; Zhang, T.; Chu, K.O.; Chu, C.Y.; Cheng, J.T.; Li, G.; He, Y.X.; Qin, L.; et al. Prodrug of green tea epigallocatechin-3-gallate (Pro-EGCG) as a potent anti-angiogenesis agent for endometriosis in mice. *Angiogenesis* **2013**, *16*, 59–69. [[CrossRef](#)] [[PubMed](#)]
23. Kopustinskiene, D.M.; Jakstas, V.; Savickas, A.; Bernatoniene, J. Flavonoids as Anticancer Agents. *Nutrients* **2020**, *12*, 457. [[CrossRef](#)] [[PubMed](#)]
24. Safe, S.; Jayaraman, A.; Chapkin, R.S.; Howard, M.; Mohankumar, K.; Shrestha, R. Flavonoids: Structure–function and mechanisms of action and opportunities for drug development. *Toxicol. Res.* **2021**, *37*, 147–162. [[CrossRef](#)] [[PubMed](#)]
25. Goya-Jorge, E.; Rodríguez, M.E.J.; Veitía, M.S.-I.; Giner, R.M. Plant Occurring Flavonoids as Modulators of the Aryl Hydrocarbon Receptor. *Molecules* **2021**, *26*, 2315. [[CrossRef](#)] [[PubMed](#)]
26. Wang, K.; Lv, Q.; Miao, Y.M.; Qiao, S.M.; Dai, Y.; Wei, Z.F. Cardamonin, a natural flavone, alleviates inflammatory bowel disease by the inhibition of NLRP3 inflammasome activation via an AhR/Nrf2/NQO1 pathway. *Biochem. Pharmacol.* **2018**, *155*, 494–509. [[CrossRef](#)] [[PubMed](#)]
27. Bae, M.-J.; Shin, H.S.; See, H.-J.; Jung, S.Y.; Kwon, D.-A.; Shon, D.-H. Baicalein induces CD4+Foxp3+ T cells and enhances intestinal barrier function in a mouse model of food allergy. *Sci. Rep.* **2016**, *6*, 32225. [[CrossRef](#)]
28. Zhao, J.; Yang, J.; Xie, Y. Improvement strategies for the oral bioavailability of poorly water-soluble flavonoids: An overview. *Int. J. Pharm.* **2019**, *570*, 118642. [[CrossRef](#)]
29. Lith, S.C.; van Os, B.W.; Seijkens, T.T.P.; de Vries, C.J.M. ‘Nur’turing tumor T cell tolerance and exhaustion: Novel function for Nuclear Receptor Nur77 in immunity. *Eur. J. Immunol.* **2020**, *50*, 1643–1652. [[CrossRef](#)]
30. Pearen, M.A.; Muscat, G.E.O. Minireview: Nuclear Hormone Receptor 4A Signaling: Implications for Metabolic Disease. *Mol. Endocrinol.* **2010**, *24*, 1891–1903. [[CrossRef](#)]
31. Safe, S.; Karki, K. The Paradoxical Roles of Orphan Nuclear Receptor 4A (NR4A) in Cancer. *Mol. Cancer Res.* **2021**, *19*, 180–191. [[CrossRef](#)] [[PubMed](#)]
32. Karki, K.; Mohankumar, K.; Schoeller, A.; Martin, G.; Shrestha, R.; Safe, S. NR4A1 Ligands as Potent Inhibitors of Breast Cancer Cell and Tumor Growth. *Cancers* **2021**, *13*, 2682. [[CrossRef](#)] [[PubMed](#)]
33. Shrestha, R.; Mohankumar, K.; Martin, G.; Hailemariam, A.; Lee, S.-O.; Jin, U.-H.; Burghardt, R.; Safe, S. Flavonoids kaempferol and quercetin are nuclear receptor 4A1 (NR4A1, Nur77) ligands and inhibit rhabdomyosarcoma cell and tumor growth. *J. Exp. Clin. Cancer Res.* **2021**, *40*, 392. [[CrossRef](#)] [[PubMed](#)]

34. Zhang, L.; Martin, G.; Mohankumar, K.; Hampton, J.T.; Liu, W.R.; Safe, S. Resveratrol Binds Nuclear Receptor 4A1 (NR4A1) and Acts as an NR4A1 Antagonist in Lung Cancer Cells. *Mol. Pharmacol.* **2022**, *102*, 80–91. [[CrossRef](#)]
35. Lee, H.-S.; Kim, S.-H.; Kim, B.-M.; Safe, S.; Lee, S.-O. Brousochalcone A Is a Novel Inhibitor of the Orphan Nuclear Receptor NR4A1 and Induces Apoptosis in Pancreatic Cancer Cells. *Molecules* **2021**, *26*, 2316. [[CrossRef](#)]
36. Park, H.; Jin, U.-H.; Martin, G.; Chapkin, R.S.; Davidson, L.A.; Lee, K.; Jayaraman, A.; Safe, S. Structure-activity relationships among mono- and dihydroxy flavones as aryl hydrocarbon receptor (AhR) agonists or antagonists in CACO2 cells. *Chem. Interactions* **2022**, *365*, 110067. [[CrossRef](#)]
37. Jin, U.-H.; Park, H.; Li, X.; Davidson, L.A.; Allred, C.; Patil, B.; Jayaprakasha, G.; Orr, A.A.; Mao, L.; Chapkin, R.S.; et al. Structure-Dependent Modulation of Aryl Hydrocarbon Receptor-Mediated Activities by Flavonoids. *Toxicol. Sci.* **2018**, *164*, 205–217. [[CrossRef](#)]
38. Zhan, Y.-Y.; Chen, Y.; Zhang, Q.; Zhuang, J.-J.; Tian, M.; Chen, H.-Z.; Zhang, L.-R.; Zhang, H.-K.; He, J.-P.; Wang, W.-J.; et al. The orphan nuclear receptor Nur77 regulates LKB1 localization and activates AMPK. *Nat. Chem. Biol.* **2012**, *8*, 897–904. [[CrossRef](#)]
39. Jordan, V.C. Antiestrogens and Selective Estrogen Receptor Modulators as Multifunctional Medicines. 1. Receptor Interactions. *J. Med. Chem.* **2003**, *46*, 883–908. [[CrossRef](#)]
40. Burris, T.P.; Solt, L.A.; Wang, Y.; Crumbley, C.; Banerjee, S.; Griffett, K.; Lundasen, T.; Hughes, T.; Kojetin, D.J. Nuclear Receptors and Their Selective Pharmacologic Modulators. *Pharmacol. Rev.* **2013**, *65*, 710–778. [[CrossRef](#)]
41. Mullican, S.E.; Zhang, S.; Konopleva, M.; Ruvolo, V.; Andreoff, M.; Milbrandt, J.; Conneely, O.M. Abrogation of nuclear receptors Nr4a3 and Nr4a1 leads to development of acute myeloid leukemia. *Nat. Med.* **2007**, *13*, 730–735. [[CrossRef](#)] [[PubMed](#)]
42. Ramirez-Herrick, A.M.; Mullican, S.E.; Sheehan, A.M.; Conneely, O.M. Reduced NR4A gene dosage leads to mixed myelodysplastic/myeloproliferative neoplasms in mice. *Blood* **2011**, *117*, 2681–2690. [[CrossRef](#)]
43. Liu, J.-J.; Zeng, H.-N.; Zhang, L.-R.; Zhan, Y.-Y.; Chen, Y.; Wang, Y.; Wang, J.; Xiang, S.-H.; Liu, W.-J.; Wang, W.-J.; et al. A Unique Pharmacophore for Activation of the Nuclear Orphan Receptor Nur77 In vivo and In vitro. *Cancer Res.* **2010**, *70*, 3628–3637. [[CrossRef](#)] [[PubMed](#)]
44. Chen, Z.; Zhang, D.; Yan, S.; Hu, C.; Huang, Z.; Li, Z.; Peng, S.; Li, X.; Zhu, Y.; Yu, H.; et al. SAR study of celastrol analogs targeting Nur77-mediated inflammatory pathway. *Eur. J. Med. Chem.* **2019**, *177*, 171–187. [[CrossRef](#)] [[PubMed](#)]
45. Jung, Y.S.; Lee, H.S.; Cho, H.R.; Kim, K.J.; Kim, J.H.; Safe, S.; Lee, S.O. Dual targeting of Nur77 and AMPK $\alpha$  by isoalantolactone inhibits adipogenesis in vitro and decreases body fat mass in vivo. *Int. J. Obes.* **2019**, *43*, 952–962. [[CrossRef](#)] [[PubMed](#)]
46. Lee, H.-S.; Safe, S.; Lee, S.-O. Inactivation of the orphan nuclear receptor NR4A1 contributes to apoptosis induction by fangchinoline in pancreatic cancer cells. *Toxicol. Appl. Pharmacol.* **2017**, *332*, 32–39. [[CrossRef](#)]
47. Hu, M.; Luo, Q.; Alitongbieke, G.; Chong, S.; Xu, C.; Xie, L.; Chen, X.; Zhang, D.; Zhou, Y.; Wang, Z.; et al. Celastrol-Induced Nur77 Interaction with TRAF2 Alleviates Inflammation by Promoting Mitochondrial Ubiquitination and Autophagy. *Mol. Cell* **2017**, *66*, 141–153.e6. [[CrossRef](#)]
48. Lakshmi, S.P.; Reddy, A.T.; Banno, A.; Reddy, R.C. Molecular, chemical, and structural characterization of prostaglandin A2 as a novel agonist for Nur77. *Biochem. J.* **2019**, *476*, 2757–2767. [[CrossRef](#)]
49. Zhou, M.; Peng, B.-R.; Tian, W.; Su, J.-H.; Wang, G.; Lin, T.; Zeng, D.; Sheu, J.-H.; Chen, H. 12-Deacetyl-12-epi-Scalaradial, a Scalarane Sesterterpenoid from a Marine Sponge *Hippospongia* sp., Induces HeLa Cells Apoptosis via MAPK/ERK Pathway and Modulates Nuclear Receptor Nur77. *Mar. Drugs* **2020**, *18*, 375. [[CrossRef](#)]
50. Li, W.; Hang, S.; Fang, Y.; Bae, S.; Zhang, Y.; Zhang, M.; Wang, G.; McCurry, M.D.; Bae, M.; Paik, D.; et al. A bacterial bile acid metabolite modulates Treg activity through the nuclear hormone receptor NR4A1. *Cell Host. Microbe* **2021**, *29*, 1366–1377.e9. [[CrossRef](#)]
51. Vinayavekhin, N.; Saghatelian, A. Discovery of a Protein–Metabolite Interaction between Unsaturated Fatty Acids and the Nuclear Receptor Nur77 Using a Metabolomics Approach. *J. Am. Chem. Soc.* **2011**, *133*, 17168–17171. [[CrossRef](#)]
52. Rajan, S.; Jang, Y.; Kim, C.-H.; Kim, W.; Toh, H.T.; Jeon, J.; Song, B.; Serra, A.; Lescar, J.; Yoo, J.Y.; et al. PGE1 and PGA1 bind to Nurr1 and activate its transcriptional function. *Nat. Chem. Biol.* **2020**, *16*, 876–886. [[CrossRef](#)]
53. Bruning, J.M.; Wang, Y.; Oltrabella, F.; Tian, B.; Kholodar, S.A.; Liu, H.; Bhattacharya, P.; Guo, S.; Holton, J.M.; Fletterick, R.J.; et al. Covalent Modification and Regulation of the Nuclear Receptor Nurr1 by a Dopamine Metabolite. *Cell Chem. Biol.* **2019**, *26*, 674–685.e6. [[CrossRef](#)] [[PubMed](#)]
54. de Vera, I.M.; Giri, P.K.; Munoz-Tello, P.; Brust, R.; Fuhrmann, J.; Matta-Camacho, E.; Shang, J.; Campbell, S.; Wilson, H.D.; Granados, J.; et al. Identification of a Binding Site for Unsaturated Fatty Acids in the Orphan Nuclear Receptor Nurr1. *ACS Chem. Biol.* **2016**, *11*, 1795–1799. [[CrossRef](#)] [[PubMed](#)]
55. Kholodar, S.A.; Lang, G.; Cortopassi, W.A.; Iizuka, Y.; Brah, H.S.; Jacobson, M.P.; England, P.M. Analogs of the Dopamine Metabolite 5,6-Dihydroxyindole Bind Directly to and Activate the Nuclear Receptor Nurr1. *ACS Chem. Biol.* **2021**, *16*, 1159–1163. [[CrossRef](#)]
56. Ponte, L.G.S.; Pavan, I.C.B.; Mancini, M.C.S.; Da Silva, L.G.S.; Morelli, A.P.; Severino, M.B.; Bezerra, R.M.N.; Simabuco, F.M. The Hallmarks of Flavonoids in Cancer. *Molecules* **2021**, *26*, 2029. [[CrossRef](#)]
57. Abotaleb, M.; Samuel, S.M.; Varghese, E.; Varghese, S.; Kubatka, P.; Liskova, A.; Büsselberg, D. Flavonoids in Cancer and Apoptosis. *Cancers* **2018**, *11*, 28. [[CrossRef](#)]

58. Xie, Y.; Tian, Y.; Zhang, Y.; Zhang, Z.; Chen, R.; Li, M.; Tang, J.; Bian, J.; Li, Z.; Xu, X. Overview of the development of selective androgen receptor modulators (SARMs) as pharmacological treatment for osteoporosis (1998–2021). *Eur. J. Med. Chem.* **2022**, *230*, 114119. [[CrossRef](#)] [[PubMed](#)]
59. D'arrigo, G.; Gianquinto, E.; Rossetti, G.; Cruciani, G.; Lorenzetti, S.; Spyrakis, F. Binding of Androgen- and Estrogen-Like Flavonoids to Their Cognate (Non)Nuclear Receptors: A Comparison by Computational Prediction. *Molecules* **2021**, *26*, 1613. [[CrossRef](#)]
60. Choi, S.Y.; Ha, T.Y.; Ahn, J.Y.; Kim, S.R.; Kang, K.S.; Hwang, I.K.; Kim, S. Estrogenic activities of isoflavones and flavones and their structure-activity relationships. *Planta Med.* **2008**, *74*, 25–32. [[CrossRef](#)]
61. Halgren, T.A.; Murphy, R.B.; Friesner, R.A.; Beard, H.S.; Frye, L.L.; Pollard, W.T.; Banks, J.L. Glide: A New Approach for Rapid, Accurate Docking and Scoring. 2. Enrichment Factors in Database Screening. *J. Med. Chem.* **2004**, *47*, 1750–1759. [[CrossRef](#)] [[PubMed](#)]
62. Friesner, R.A.; Murphy, R.B.; Repasky, M.P.; Frye, L.L.; Greenwood, J.R.; Halgren, T.A.; Sanschagrin, P.C.; Mainz, D.T. Extra precision glide: Docking and scoring incorporating a model of hydrophobic enclosure for protein-ligand complexes. *J. Med. Chem.* **2006**, *49*, 6177–6196. [[CrossRef](#)] [[PubMed](#)]
63. Friesner, R.A.; Banks, J.L.; Murphy, R.B.; Halgren, T.A.; Klicic, J.J.; Mainz, D.T.; Repasky, M.P.; Knoll, E.H.; Shelley, M.; Perry, J.K.; et al. Glide: A new approach for rapid, accurate docking and scoring. 1. Method and assessment of docking accuracy. *J. Med. Chem.* **2004**, *47*, 1739–1749. [[CrossRef](#)] [[PubMed](#)]

**Disclaimer/Publisher's Note:** The statements, opinions and data contained in all publications are solely those of the individual author(s) and contributor(s) and not of MDPI and/or the editor(s). MDPI and/or the editor(s) disclaim responsibility for any injury to people or property resulting from any ideas, methods, instructions or products referred to in the content.